



Nonlinear saturation of mirror instability

Hongpeng Qu,¹ Zhihong Lin,¹ and Liu Chen¹

Received 7 March 2008; revised 9 April 2008; accepted 21 April 2008; published 30 May 2008.

[1] Mechanism of the nonlinear saturation of compressible electromagnetic mirror instability is studied using the gyrokinetic particle simulation. Phase-space particle trapping due to the mirror force is found to be the dominant saturation mechanism in the simulation of a single mirror mode with relatively weak drive. At the nonlinear saturation, the phase-space island of the distribution function is formed. The oscillation frequency of the saturated perturbation amplitude is close to the bounce frequency of the trapped particles, which is comparable to the linear growth rate of the mirror mode. Scaling of the saturation amplitude is consistent with the onset of the particle trapping. With strong instability drive, relaxation toward marginal stability dominates the nonlinear saturation of the mirror instability. Phase-space trapping, however, persists after the saturation and continues to regulate the nonlinear evolution of the mirror mode.
Citation: Qu, H., Z. Lin, and L. Chen (2008), Nonlinear saturation of mirror instability, *Geophys. Res. Lett.*, 35, L10108, doi:10.1029/2008GL033907.

1. Introduction

[2] Mirror instability is a low frequency compressible electromagnetic mode driven by temperature anisotropy in high- β plasmas (β is the ratio between kinetic and magnetic pressure). It has been observed by satellites in space plasmas, such as planetary and cometary magnetosheaths [Rae *et al.*, 2007; Joy *et al.*, 2006]. In such environments, the perpendicular temperature often exceeds the parallel temperature, i.e., $T_{\perp} > T_{\parallel}$, and the magnetic mirror instability at very low frequency $\omega \ll k_{\parallel} v_i$ can be excited by the temperature anisotropy (Here, v_i is the ion thermal velocity and k_{\parallel} is the wave vector parallel to the magnetic field).

[3] This instability has attracted considerable interest because of its probable importance in contributing to the low-frequency compressible magnetic turbulence in the magnetized plasmas. Much attention has been paid to the kinetic analysis of the linear growth of the mirror mode under various conditions [Southwood and Kivelson, 1993; Pokhotelov *et al.*, 2003]. These kinetic analyses in the long wavelength limit found that the wave-particle resonance plays a crucial role in driving the mirror instability. Because of the observation of the short wavelength mirror structures in the Earth magnetosheath where the perpendicular wavelength is in the same order as ion Larmor radius [Takahashi, 1988; Sahraoui *et al.*, 2006], the effects of the finite Larmor radius (FLR) have been discussed

using the Vlasov theory [Hasegawa, 1969; Pokhotelov *et al.*, 2004], the fluid model [Passot and Sulem, 2006], and the gyrokinetic theory [Qu *et al.*, 2007]. These kinetic studies showed that the FLR effects limit the linear growth of the short wavelength mirror mode. The nonlinear evolution of the mirror instability has also been studied numerically and qualitatively. McKean *et al.* [1993] showed that the temperature anisotropy of the plasma drops after the saturation of the mirror instability. The nonlinear FLR effects [Kuznetov *et al.*, 2007] and particle trapping [Pokhotelov *et al.*, 2008] on the saturation of the mirror instability have recently been discussed. In works of Kivelson and Southwood [1996] and Pantellini [1998], the nonlinear saturation of the mirror mode is explained as a relaxation to the locally marginal stability. In their analysis, the particles are divided into the trapped particles and the untrapped particles. In the region where the magnetic field magnitude increases, the trapped particles are excluded from the rising field region by the mirror force. This process produces a decrease in the kinetic pressure and thus the β value, allowing the marginally stable state to be achieved in the strong field region. In the center of magnetic field well, the trapped particles are cooled by losing perpendicular energy because the magnetic field strength is decreasing and the magnetic moment is conserved. In this way, the perpendicular temperature and thus temperature anisotropy decrease, the linear growth of the mirror instability can thus be stabilized by the relaxation to a marginal stability in the weak field region.

[4] Despite all these studies, the understanding of the nonlinear physics of the mirror instability remains limited. It is desirable to develop a kinetic theory with a transparent physics picture that also provides an efficient tool for the nonlinear studies of the mirror instability, both analytically and computationally. Here we adopt the gyrokinetic approach where the fast gyromotion is removed [Frieman and Chen, 1982; Brizard, 1989]. In our work, a gyrokinetic particle-in-cell (PIC) simulation model [Lee, 1987] for the compressible electromagnetic turbulence has been developed [Qu *et al.*, 2007; Qu and Lin, 2008]. The linear benchmark of the mirror instability shows that the simulation results match well with the analytical results [Qu *et al.*, 2007]. From the nonlinear simulation of a single mirror mode, we find a new saturation mechanism of the mirror instability. Our simulation results show that the phase-space trapping of the ions plays a dominant role in the saturation of the mirror instability when the instability drive is relatively weak. Our simulation results also show that the dominant saturation mechanism is the relaxation to the marginal stability when the drive is very strong. However, after the relaxation to the marginal stability, the phase-space trapping persists and continues to regulate the nonlinear dynamics of the mirror modes.

¹Department of Physics and Astronomy, University of California, Irvine, California, USA.

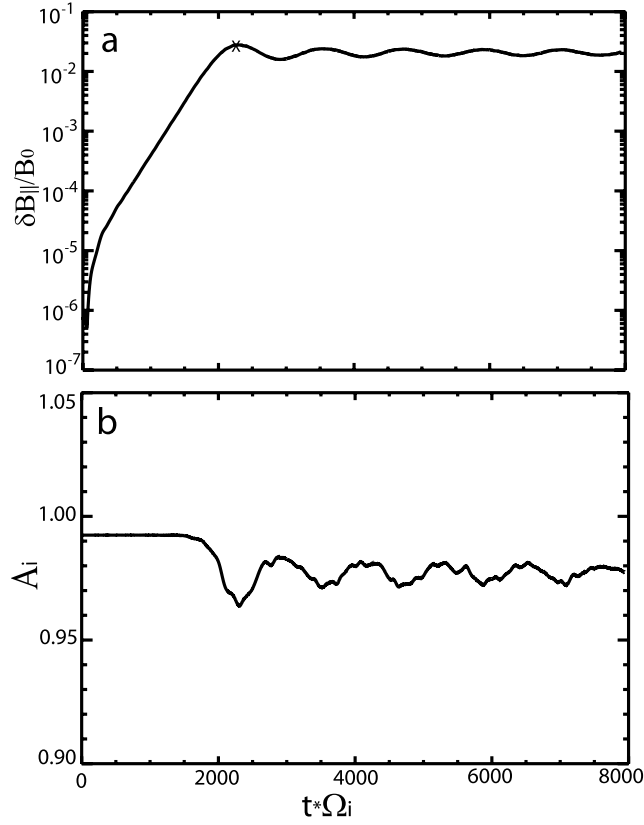


Figure 1. Time history of the amplitude of (a) the perturbed parallel magnetic field and (b) the ion temperature anisotropy for $\beta_{i,\perp} = 2$ and $A_i = 1$.

[5] This paper is organized as follows. Section 2 describes the gyrokinetic PIC simulation model. In section 3 we present the nonlinear simulation results and discuss the saturation mechanism of the mirror instability. Section 4 is the summary.

2. Nonlinear Gyrokinetic Particle Simulation Model

[6] The gyrokinetic theory is a powerful tool for the nonlinear analysis and simulation of the low-frequency instabilities. It employs the gyrokinetic ordering as

$$\frac{\omega}{\Omega_i} \sim \frac{\rho_i}{L} \sim k_{\parallel} \rho_i \sim \frac{\delta B}{B} \sim \varepsilon$$

$$k_{\perp} \rho_i \sim 1. \quad (1)$$

Here, $\Omega_i = qB_0/m_i c$ and $\rho_i = v_{i,\perp}/\Omega_i$ are, respectively, the ion cyclotron frequency and Larmor radius, L is the macroscopic background plasma scale length, k_{\parallel} and k_{\perp} are the parallel and perpendicular wave vectors, δB and B are the perturbed and total magnetic field, and ε is a smallness parameter. Using such ordering, we can remove the explicit dependence of the Vlasov equation on the gyrophase to reduce the dimensions of the phase space from six to five, while retaining the FLR effects and the nonlinear wave-particle interactions. In particular, by eliminating the gyromotion of particles and the associated high frequency modes, we can use much larger time steps to increase the

computation efficiency and to reduce the particle noise in the nonlinear simulation.

[7] In this work, the nonlinear study of the mirror instability in the uniform plasma and equilibrium magnetic field has been carried out using the gyrokinetic particle-in-cell simulations. The gyrokinetic equation in this simple equilibrium is [Brizard, 1989]

$$\frac{\partial \delta F_i}{\partial t} + (\bar{U} \mathbf{b} + \dot{\bar{\mathbf{X}}}_{\perp}) \nabla \delta F_i + \dot{\bar{\rho}}_{\parallel} \frac{\partial \delta F_i}{\partial \bar{\rho}_{\parallel}} = -\dot{\bar{\rho}}_{\parallel} \frac{\partial F_{0i}}{\partial \bar{\rho}_{\parallel}} \quad (2)$$

where $\delta F_i(\bar{\mathbf{X}}, \bar{\rho}_{\parallel}, \bar{\mu})$ is the perturbed distribution function of ions in the reduced five-dimensional gyrocenter phase space, $\bar{\mathbf{X}}$ is the gyrocenter position, $\bar{\rho}_{\parallel} = \bar{U}/\Omega_i$, \bar{U} is the gyrocenter parallel velocity, $\bar{\mu} = \bar{v}_{\perp}^2/2B$ is the adiabatic invariant. The kinetic effects of electrons on the mirror instability are neglected when assuming $T_e/T_i \ll 1$ in this work. The equations of motion for ion gyrocenters in equation (2) are

$$\frac{d\bar{X}_{\parallel}}{dt} = \bar{U} = \bar{\rho}_{\parallel} \Omega_i, \quad (3)$$

$$\frac{d\bar{\mathbf{X}}_{\perp}}{dt} = \frac{c}{B_0} \mathbf{b} \times \nabla \langle \delta \varphi - \frac{1}{c} \mathbf{v} \cdot \delta \mathbf{A} \rangle, \quad (4)$$

$$\dot{\bar{\rho}}_{\parallel} = \frac{\dot{\bar{U}}}{\Omega_i} = -\frac{q}{\Omega_i m} \mathbf{b} \cdot \nabla \langle \delta \varphi - \frac{1}{c} \mathbf{v} \cdot \delta \mathbf{A} \rangle, \quad (5)$$

where $\langle \dots \rangle = 1/2\pi \int_0^{2\pi} (\dots) d\zeta$ represents gyro-averaging. Here, $\delta \varphi$ and $\delta \mathbf{A}$ are the perturbed scalar and vector potentials, respectively. In order to advance δF_i , we need to calculate $\delta \varphi$, $\delta A_{\parallel} = \mathbf{b} \cdot \delta \mathbf{A}$ and $\delta B_{\parallel} = i(\mathbf{b} \times \mathbf{k}_{\perp}) \cdot \delta \mathbf{A}$ from the Poisson equation and Ampere's law. Here, to focus on the basic physics of the mirror instability, we keep only the dominant effects of the perturbed parallel magnetic field δB_{\parallel} . Therefore, we only need the perpendicular Ampere's law [Qu et al., 2007; Qu and Lin, 2008]

$$-\frac{i\delta j_{y0}}{ck_{\perp}} + \frac{\delta B_{\parallel}}{4\pi} = -\frac{k_{\parallel}^2}{k_{\perp}^2} \left[1 + \alpha_b \cdot (\beta_{\perp} - \beta_{\parallel}) \right] \frac{\delta B_{\parallel}}{4\pi}, \quad (6)$$

$$\delta j_{y0} = q_i \int v_y \delta F_i d\mathbf{v} + i\delta B_{\parallel} \frac{2nT_{i,\perp} ck_{\perp}}{B_0^2} e^{-k_{\perp}^2 \rho_i^2/2} \times [I_0(k_{\perp}^2 \rho_i^2/2) - I_1(k_{\perp}^2 \rho_i^2/2)] \quad (7)$$

where $\alpha_b = \int_{-\infty}^{+\infty} dv_{\parallel} \int_0^{+\infty} v_{\perp} dv_{\perp} \cdot 4\pi \frac{q^2}{m} \frac{\partial F}{\partial \mu} \frac{v_{\parallel}^2 v_{\perp}^2}{\Omega^2 c^2} (J_1')^2$, I_0 and I_1 are modified Bessel functions. Here, the second term on the right side of equation (7) comes from the perpendicular gyrocenter drift.

[8] Because we assume the uniform plasma and magnetic field, our simulation model can employ a periodic system in the $x - z$ plane with simulation axis along \mathbf{x} and \mathbf{z} , the equilibrium magnetic field $\mathbf{B}_0 = B_0 \mathbf{e}_z$. The size of the simulation box is determined by the value of $k_{\perp} \rho_i$ and k_{\parallel}/k_{\perp} where $\mathbf{k} = k_{\perp} \mathbf{e}_x + k_{\parallel} \mathbf{e}_z$. The normalized simulation box length perpendicular to the magnetic field is $\hat{L}_x = 2\pi/(k_{\perp} \rho_i)$, which is equal to the perpendicular wavelength of the mode calculated in the simulation. Accordingly, the

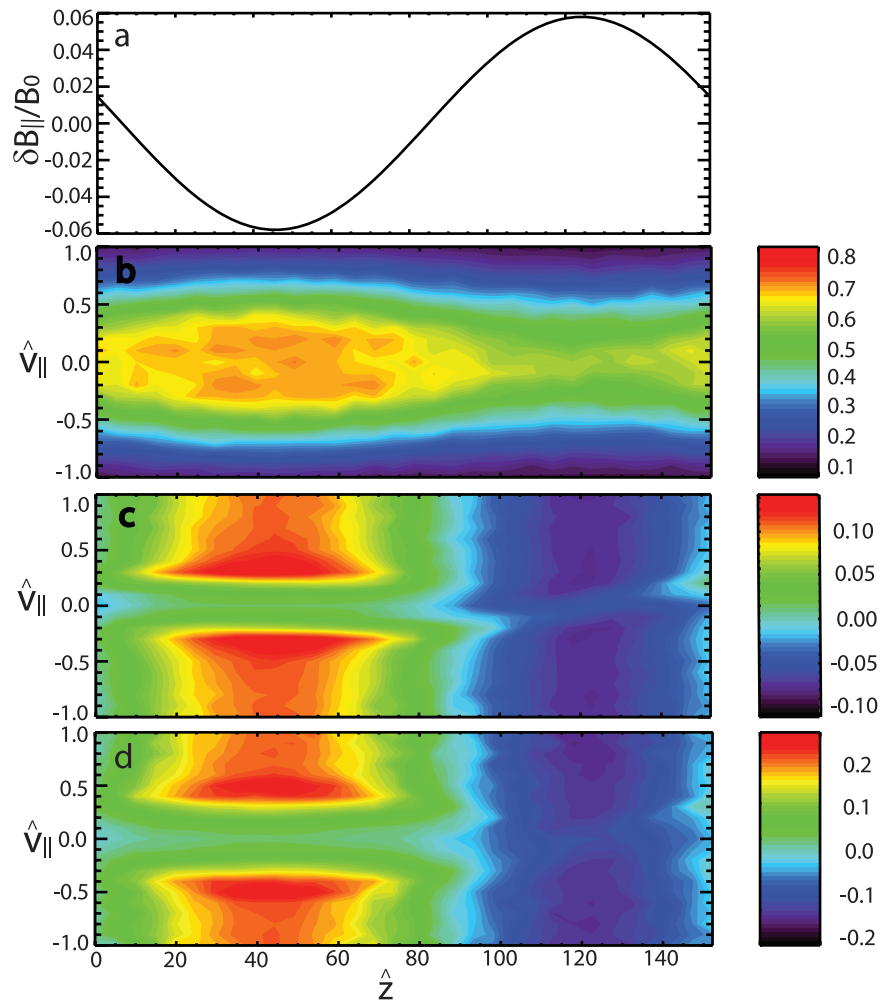


Figure 2. The island formation of the distribution function in the phase-space at $t^* \Omega_i = 2250$ (the cross in Figure 1a). (a) The amplitude of the perturbed parallel magnetic field. (b) The distribution function $f = f_0 + \delta F_i$ in the phase-space. (c and d) The normalized perturbed distribution function $\delta F_i/f_0$ taken for $\hat{\mu} = 1$ and $\hat{\mu} = 2$, respectively.

parallel length of simulation box is $\hat{L}_z = \hat{L}_x/(k_{\parallel}/k_{\perp})$. The simulation domain is discretized by a set of grids in both x and z directions and the positions of ions are loaded uniformly in the cells with the Bi-Maxwellian distribution in the velocity space. Because the perturbed magnetic field in the simulation box is periodic by the box length, the field quantities at one end of the box are the same as the quantities on the other end. The positions and velocities of the ion gyrocenters are advanced by the second-order Runge-Kutta scheme. Consistent with the periodic boundary condition, we insert an ion with same velocity at one end of the simulation box whenever it escapes from the other end. The perpendicular Ampere's law is solved in k -space using the fast Fourier transform (FFT).

[9] The gyrokinetic simulation of the mirror instability starts from the linear case [Qu *et al.*, 2007] where only the first order terms of small quantity ε in equation (2) are kept in simulation. It is important to make sure that the numerical noise associated with discreteness in phase space does not affect the physics being studied. In this regard, the numerical convergence with respect to the number of particles, the number of grids and the time step in simulation has been achieved. The gyrokinetic PIC simulation results match well with the analytical results of the linear dispersion relation.

Building on the convergence study and the linear benchmark of the gyrokinetic PIC simulation, we can perform the nonlinear simulation of the mirror instability by keeping the second order terms of small quantity ε in equation (2).

3. Nonlinear Simulation Results

[10] Before studying the complicated compressible electromagnetic turbulence, we carried out first the nonlinear simulation of a single mode to study the basic physics of the mirror instability. Here, we keep $\beta_{i,\perp} = 2$ and $A_i = T_{\perp}/T_{\parallel} - 1 = 1$ and choose $k_{\perp}\rho_i = 0.2$ and $k_{\parallel}/k_{\perp} = 0.2$.

[11] Figure 1 shows the time history of the amplitude of the perturbed parallel magnetic field (Figure 1a) and the ion temperature anisotropy A_i (Figure 1b) in the nonlinear simulation. In Figure 1a, the exponential growth of the amplitude of the perturbed magnetic field indicates the linear phase in the early part of this graph with a linear growth rate $\gamma/\Omega_i \approx 0.0043$. It is followed by the nonlinear saturation of the mirror mode at $t^* \Omega_i = 2250$, the oscillation of the amplitude of the perturbed parallel magnetic field can be found after the saturation. In Figure 1b, it shows that the temperature anisotropy

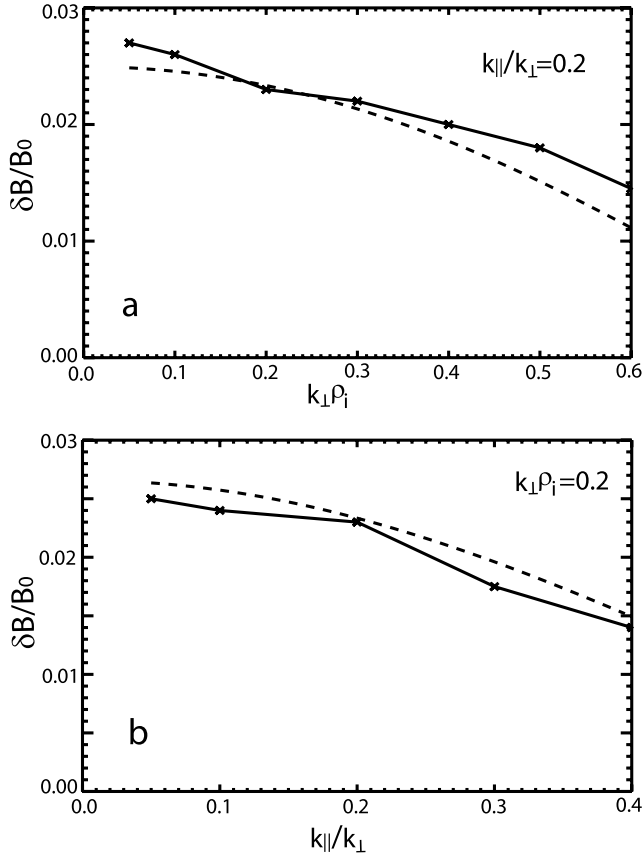


Figure 3. Saturated amplitude of the perturbed magnetic field with respect to (a) $k_{\perp}\rho_i$ and (b) k_{\parallel}/k_{\perp} . The continuous lines show our simulation results and the dashed lines are the best fit using equation (11).

decreases less than 2% after the saturation. This means that the previously introduced nonlinear saturation mechanism of the relaxation to the marginal stability does not work here. This result indicates that there exists another nonlinear saturation mechanism for the mirror instability. In fact, the nonlinear oscillation of the perturbed field amplitude in Figure 1a provides an important clue. From Figure 1a, we can calculate the oscillation frequency of the amplitude of the perturbed parallel magnetic field $\omega_{nl}/\Omega_i \approx 0.0054$. We can also find that the saturation amplitude $\delta B_{\parallel}/B_0 \approx 0.023$. From the motion equation of the trapped particles in the magnetic well, $m\ddot{x} = -\mu\nabla_{\parallel}\delta B$, we obtain the bounce frequency of the trapped particles under such amplitude of the perturbed magnetic field

$$\omega_b/\Omega_i = \left(k_{\parallel}^2 \frac{\mu B_0}{\Omega_i^2} \frac{\delta B_{\parallel}}{B_0} \right)^{1/2} = \frac{k_{\parallel}}{k_{\perp}} k_{\perp} \rho_i \sqrt{\frac{\delta B_{\parallel}}{2B_0}} = 0.0043. \quad (8)$$

According to the parameters adopted, we also know that the linear growth rate of this mode is $\gamma/\Omega_i \approx 0.0043$ from the linear gyrokinetic theory [Qu *et al.*, 2007],

$$\gamma/\Omega_i = \frac{k_{\parallel}}{k_{\perp}} k_{\perp} \rho_i \frac{-\Lambda + \beta^* A_i}{\sqrt{\pi} \beta^* (1 + A_i)^{3/2}} \quad (9)$$

where $\beta_{\perp}^* = \beta_{\perp} e^{-k_{\perp}^2 \rho_i^2/2} [I_0(k_{\perp} \rho_i) - I_1(k_{\perp} \rho_i)]$, $\Lambda = 1 + k_{\parallel}^2/k_{\perp}^2 \cdot [1 + \alpha_b (\beta_{\perp} - \beta_{\parallel})]$. We find that the nonlinear oscillation frequency of the mirror mode is close to the bounce frequency of the trapped particles and the linear growth rate of the mode, i.e.,

$$\omega_{nl} \sim \omega_b \sim \gamma. \quad (10)$$

This result is similar to O'Neil's [1965] work about the collisionless damping of the nonlinear plasma oscillation due to the parallel electric field. Equation (10) indicates that the phase-space trapping due to the mirror force determines the nonlinear saturation process of the mirror mode.

[12] Figure 2 shows the island formation of the distribution function of the ions in the phase-space $(\hat{v}_{\parallel}, \hat{z})$ where $\hat{v}_{\parallel} = v_{\parallel}/v_{t,\perp}$ is the normalized parallel velocity and $\hat{z} = z/\rho_i$ is the normalized position of the ion along \mathbf{B}_0 . Figure 2 is taken at the nonlinear saturation (shown in Figure 1a by the cross). Figure 2b shows that an island of the distribution function $f = f_0 + \delta F_i$ is formed in the phase-space indicating the onset of the particle trapping. Here, f_0 and δF_i are the equilibrium and perturbed distribution functions of ions, respectively. The center of the island lies at $\hat{v}_{\parallel} = 0$, indicating that the phase velocity of the mode is zero.

[13] From the gyrokinetic equations of equations (2)–(5), there are qualitative predictions that $\delta F_i/f_0$ increases with the magnetic moment μ and that maximum $\delta F_i/f_0$ can be found for the barely trapped particles. Figures 2c and 2d show the

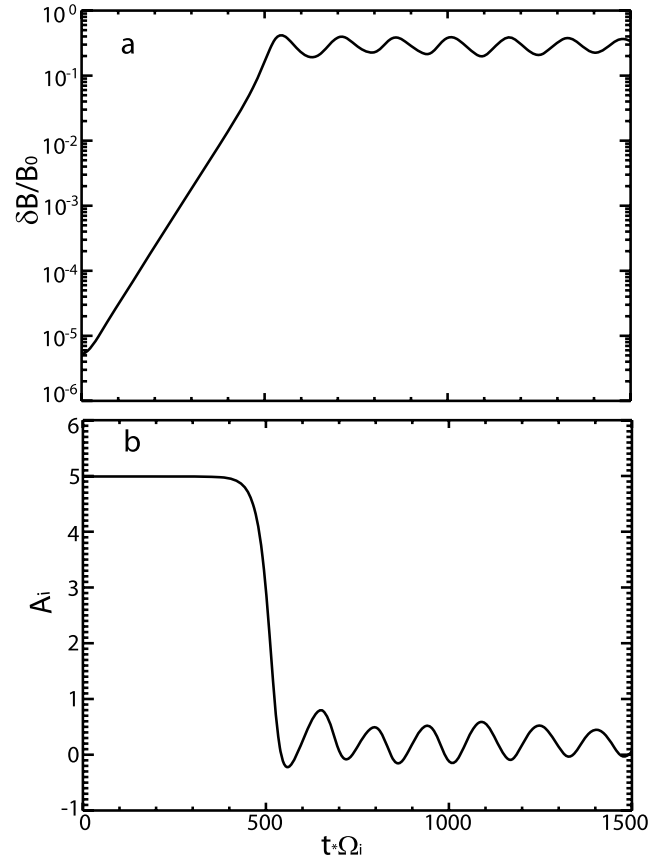


Figure 4. Time history of the amplitude of (a) the perturbed parallel magnetic field and (b) the ion temperature anisotropy for $\beta_{i,\perp} = 12$ and $A_i = 5$.

normalized perturbed distribution function $\delta F_i/f_0$ of ions with different normalized perpendicular energy $\hat{\mu} = \mu B/T_{\perp}$. For the case of $\hat{\mu} = 2$ in Figure 2d, the amplitude of $\delta F_i/f_0$ is just two times larger than that in Figure 2c for the case of $\hat{\mu} = 1$. Furthermore, in Figure 2d, the maximal $\delta F_i/f_0$ is at $\hat{v}_{\parallel} \sim 0.45$ and about 1.4 times larger than the $\hat{v}_{\parallel} \sim 0.32$ for the case of $\hat{\mu} = 1$. This result is consistent with the prediction from the condition $\mu\delta B_{\parallel} = mv_{\parallel}^2/2$ of the barely trapped particles. These results in Figure 2 verify our theory that the phase-space trapping plays the dominant role in the nonlinear saturation of the mirror instability.

[14] From equations (8)–(10), we can estimate the amplitude of the saturation by assuming saturation occurs when $\omega_b = C\gamma$ with constant C to be determined, i.e.,

$$\frac{\delta B_{\parallel}}{B_0} \sim 2 \cdot \left[\frac{\beta_{\perp}^* A_i - \Lambda}{\sqrt{\pi}(1 + A_i)^{3/2} \beta_{\perp}^*} \right]^2 \cdot C. \quad (11)$$

To find out the value of C , we have performed parameter scan for k_{\parallel}/k_{\perp} and $k_{\perp}\rho_i$ as shown in Figure 3. It shows that the amplitude of saturation calculated from equation (11) matches well with our simulation results for $C = 1.42$ using a least-squared-fit method for both panels of Figure 3. Again it verifies our explanation of the nonlinear saturation via the phase-space trapping.

[15] However, for the strong drive case when $\beta_{i,\perp}$ and A_i are much larger than 1, the situation is different. For the nonlinear simulation using $\beta_{i,\perp} = 12$ and $A_i = 5$, Figure 4 shows that temperature anisotropy drops dramatically after the saturation. This may look superficially consistent with the previous finding of saturation through relaxation to the marginal stability theory. We find that there still exists the nonlinear oscillation of the amplitude of the perturbed parallel magnetic field after the saturation. Therefore, the phase-space trapping continues to regulate the nonlinear dynamics of the mirror mode. More importantly, since the relaxation to the marginal stability is a transient process in the simulation, the relevance of this mechanism to observations is questionable.

4. Summary

[16] In this paper, we have discussed the nonlinear saturation mechanisms of the mirror instability by using the gyrokinetic particle simulation. Our simulation results show that the amplitude of the temperature anisotropy does not drop significantly at the saturation in the weak drive case. This is not consistent with the previously invoked theory of the relaxation to the marginal stability. By studying the saturation amplitude and the nonlinear oscillation frequency of the perturbed parallel magnetic field after the saturation, we find that nonlinear oscillation frequency is close to the phase-space bounce frequency of the trapped particles and the linear growth rate of the mode. Therefore the amplitude of saturation can be predicted from the expression of the linear growth rate and the phase-space bounce frequency. Furthermore, the simulation result shows the formation of the phase-space island of the distribution function. All these results indicate that the mechanism of the phase-space trapping is dominant in the nonlinear saturation of the mirror instability. In the strong drive case, we find that the amplitude of the temperature anisotropy drops significantly to satisfy the marginal stability condition.

However, after the saturation, the phase-space trapping continues to regulate the nonlinear evolution of the mirror structure. These results suggest that there are different saturation mechanisms in the different conditions and the phase-space trapping plays an important role in the nonlinear saturation of the mirror instability.

[17] In future nonlinear gyrokinetic simulation, we will study the mirror instability in nonuniform plasmas and with finite temperature ratio between ions and electrons, and multi-mode nonlinear interactions. These comprehensive simulations with realistic parameters would enable direct comparisons of simulation results with space plasma observations.

[18] **Acknowledgments.** This work is supported by an NSF CAREER award, grant ATM-0449606, an NSF grant ATM-033527, and Department of Energy (DOE) grants DE-FG02-07ER54916 and DE-FG03-94ER54736.

References

- Brizard, A. (1989), Nonlinear gyrokinetic Maxwell-Vlasov equations using magnetic co-ordinates, *J. Plasma Phys.*, *41*, 541.
- Frieman, E. A., and L. Chen (1982), Nonlinear gyrokinetic equations for low-frequency electromagnetic waves in general plasma equilibria, *Phys. Fluids*, *25*, 502.
- Hasegawa, A. (1969), Drift mirror instability in magnetosphere, *Phys. Fluids*, *12*, 2642.
- Joy, S. P., M. G. Kivelson, R. J. Walker, K. K. Khurana, C. T. Russell, and W. R. Paterson (2006), Mirror mode structures in the Jovian magnetosheath, *J. Geophys. Res.*, *111*, A12212, doi:10.1029/2006JA011985.
- Kivelson, M. G., and D. J. Southwood (1996), Mirror instability II: The mechanism of nonlinear saturation, *J. Geophys. Res.*, *101*, 17,365.
- Kuznetsov, E. A., T. Passot, and P. L. Sulem (2007), Dynamical model for nonlinear mirror modes near threshold, *Phys. Rev. Lett.*, *98*, 235003.
- Lee, W. W. (1987), Gyrokinetic particle simulation model, *J. Comput. Phys.*, *72*, 243.
- McKean, M. E., S. P. Gary, and D. Winske (1993), Kinetic physics of the mirror instability, *J. Geophys. Res.*, *98*, 21,313.
- O'Neil, T. (1965), Collisionless damping of nonlinear plasma oscillations, *Phys. Fluids*, *8*, 2255.
- Pantellini, F. G. E. (1998), A model of the formation of stable nonpropagating magnetic structures in the solar wind based on the nonlinear mirror instability, *J. Geophys. Res.*, *103*, 4789.
- Passot, T., and P. L. Sulem (2006), A fluid model with finite Larmor radius effects for mirror mode dynamics, *J. Geophys. Res.*, *111*, A04203, doi:10.1029/2005JA011425.
- Pokhotelov, O. A., I. Sandberg, R. Z. Sagdeev, R. A. Treumann, O. G. Onishchenko, M. A. Balikhin, and V. P. Pavlenko (2003), Slow drift mirror modes in finite electron-temperature plasma: Hydrodynamic and kinetic drift mirror instabilities, *J. Geophys. Res.*, *108*(A3), 1098, doi:10.1029/2002JA009651.
- Pokhotelov, O. A., R. Z. Sagdeev, M. A. Balikhin, and R. A. Treumann (2004), Mirror instability at finite ion-Larmor radius wavelengths, *J. Geophys. Res.*, *109*, A09213, doi:10.1029/2004JA010568.
- Pokhotelov, O. A., R. Z. Sagdeev, M. A. Balikhin, O. G. Onishchenko, and V. N. Fedun (2008), Nonlinear mirror waves in non-Maxwellian space plasmas, *J. Geophys. Res.*, *35*, A04225, doi:10.1029/2007JA012642.
- Qu, H., and Z. Lin (2008), Gyrokinetic particle simulation of compressional electromagnetic modes, *Commun. Comput. Phys.*, *4*, 519.
- Qu, H., Z. Lin, and L. Chen (2007), Gyrokinetic theory and simulation of mirror instability, *Phys. Plasmas*, *14*, 042108.
- Rae, I. J., I. R. Mann, C. E. J. Watt, L. M. Kistler, and W. Baumjohann (2007), Equator-S observations of drift mirror mode waves in the dawn-side magnetosphere, *J. Geophys. Res.*, *112*, A11203, doi:10.1029/2006JA012064.
- Sahraoui, F., et al. (2006), Anisotropic turbulent spectra in the terrestrial magnetosheath as seen by the Cluster spacecrafts, *Phys. Rev. Lett.*, *96*, 075002.
- Southwood, D. J., and M. G. Kivelson (1993), Mirror instability: 1. Physical mechanism of linear instability, *J. Geophys. Res.*, *98*, 9181.
- Takahashi, K. (1988), Multisatellite studies of ULF waves, *Adv. Space Res.*, *8*(9), 427.

L. Chen, Z. Lin, and H. Qu, Department of Physics and Astronomy, University of California, Irvine, CA 92697, USA. (zhihongl@uci.edu)